

# Depth-Dependent Solvent Relaxation in Membranes: Wavelength-Selective Fluorescence as a Membrane Dipstick

Amitabha Chattopadhyay\* and Sushmita Mukherjee†

Centre for Cellular & Molecular Biology, Uppal Road, Hyderabad 500 007, India

Received November 3, 1998

Membrane penetration depth represents an important parameter which can be used to define the conformation and topology of membrane proteins and probes. We have previously characterized a set of fluorescence spectroscopic approaches, collectively referred to as wavelength-selective fluorescence, as a powerful tool to monitor microenvironments in the vicinity of reporter fluorophores embedded in the membrane. Since several membrane parameters that characterize local environments such as polarity, fluidity, segmental motion, degree of water penetration, and the ability to form hydrogen bonds are known to vary as a function of depth of penetration into the membrane, we propose that wavelength-selective fluorescence could provide a novel approach to investigate the depth of membrane penetration of a reporter fluorophore. We test this hypothesis by demonstrating that chemically identical fluorophores, varying solely in terms of their localization at different depths in the membrane, experience very different local environments, as judged by wavelength-selective fluorescence parameters. We used two anthroyloxy stearic acid derivatives where the anthroyloxy group has previously been found to be either shallow (2-AS) or deep (12-AS). Our results show that the anthroyloxy moiety of 2- and 12-AS experiences different local membrane microenvironments, as reflected by varying extents of red-edge excitation shift (REES) as well as varying degrees of wavelength dependence of fluorescence polarization and lifetime and rotational correlation times. We attribute these results to differential rates of solvent reorientation in the immediate vicinity of the anthroyloxy group as a function of its membrane penetration depth. We thus provide evidence, for the first time, of depth-dependent solvent relaxation which can be used as a membrane dipstick.

## Introduction

Biological membranes are complex assemblies of lipids and proteins that allow cellular compartmentalization and act as the interface through which cells communicate with each other and with the external milieu. The biological membrane constitutes the site of many important cellular functions. However, our understanding of these processes at the molecular level is limited by the lack of high-resolution three-dimensional structures of membrane-bound molecules. It is extremely difficult to crystallize membrane-bound molecules for diffraction studies. Only a few years ago was the first complete X-ray crystallographic analysis of an integral membrane protein successfully carried out.<sup>1</sup> Even high-resolution NMR methods have limited applications for membrane-bound molecules because of slow reorientation times in membranes.<sup>2</sup>

Due to the inherent difficulty in crystallizing membrane-bound molecules, most structural analyses of such molecules have utilized other biophysical techniques with an emphasis on spectroscopic approaches. One such analysis involves determination of membrane penetration depth which usually refers to the location of a molecule or a specific site within a molecule in relation to the membrane surface. Membrane penetration depth thus constitutes an important parameter which, in the absence of a crystallographic database for membrane-bound molecules, could be used very effectively to define the conformation

and topology of membrane proteins and probes,<sup>3–13</sup> by providing one or more specific reference points in the membrane relative to which the rest of the molecule can be mapped.<sup>14–16</sup> One of us has previously developed an elegant method, known as the parallax method, for measurement of membrane penetration depth utilizing fluorescence quenching by spin-labeled (or brominated) phospholipids.<sup>5</sup> The method involves determination of the parallax in the apparent location of fluorophores detected when quenching by phospholipids spin-labeled at two different depths is compared. This method has been used to determine the penetration depths of the fluorescent nitrobenzoxadiazol (NBD) groups in a series of NBD-labeled lipids,<sup>5,9</sup> and of the membrane-embedded tryptophan residues in the reconstituted nicotinic acetylcholine

(3) London, E. *Mol. Cell. Biochem.* **1982**, *45*, 181.

(4) Blatt, E.; Sawyer, W. H. *Biochim. Biophys. Acta* **1985**, *822*, 43.

(5) Chattopadhyay, A.; London, E. *Biochemistry* **1987**, *26*, 39; Chattopadhyay, A. *J. Biosci.* **1990**, *15*, 143; Chattopadhyay, A. In *Biomembrane Structure and Function: The State of the Art*; Gaber, B. P., Easwaran, K. R. K., Eds.; Adenine Press: Schenectady, New York, 1992; p 153.

(6) Lala, A. K.; Dixit, R. R.; Koppaka, V.; Patel, S. *Biochemistry* **1988**, *27*, 8981.

(7) London, E. *Biophys. J.* **1994**, *67*, 1368.

(8) Abrams, F. S.; London, E. *Biochemistry* **1992**, *31*, 5312.

(9) Abrams, F. S.; London, E. *Biochemistry* **1993**, *32*, 10826.

(10) Abrams, F. S.; Chattopadhyay, A.; London, E. *Biochemistry* **1992**, *31*, 5322.

(11) Ghosh, A., K.; Rukmini, R.; Chattopadhyay, A. *Biochemistry* **1997**, *36*, 14291.

(12) Asuncion-Punzalan, E.; London, E. *Biochemistry* **1995**, *34*, 11460.

(13) Kachel, K.; Asuncion-Punzalan, E.; London, E. *Biochemistry* **1995**, *34*, 15475.

(14) Meers, P. *Biochemistry* **1990**, *29*, 3325.

(15) Chattopadhyay, A.; McNamee, M. G. *Biochemistry* **1991**, *30*, 7159.

(16) Everett, J.; Zlotnick, A.; Tennyson, J.; Holloway, P. W. *J. Biol. Chem.* **1986**, *261*, 6725.

† Present address: Department of Biochemistry, Cornell University Medical College, 1300 York Avenue, New York, NY 10021.

\* Address correspondence to this author. Telephone: +91-40-7172241. Fax: +91-40-7171195. E-mail: amit@ccmb.ap.nic.in.

(1) Deisenhofer, J.; Epp, O.; Miki, K.; Huber, R.; Michel, H. *Nature* **1985**, *318*, 618.

(2) Opella, S. J. *Nature Struct. Biol.* **1997**, *4* (NMR Suppl.), 845.

receptor,<sup>15</sup> in membrane-bound annexins,<sup>14</sup> and in the hemolytic peptide melittin.<sup>11</sup>

**The Wavelength-Selective Fluorescence Approach.** We have previously shown that the wavelength-selective fluorescence approach serves as a powerful tool to monitor organization and dynamics of membrane-bound probes and peptides. Wavelength-selective fluorescence comprises a set of approaches based on the red-edge effect in fluorescence spectroscopy which can be used to directly monitor the environment and dynamics around a fluorophore in a complex biological system.<sup>17</sup> A shift in the wavelength of maximum fluorescence emission toward higher wavelengths, caused by a shift in the excitation wavelength toward the red edge of absorption band, is termed red edge excitation shift (REES). This effect is mostly observed with polar fluorophores in motionally restricted media such as very viscous solutions or condensed phases where the dipolar relaxation time for the solvent shell around a fluorophore is comparable to or longer than its fluorescence lifetime.<sup>17–20</sup> REES arises from slow rates of solvent relaxation (reorientation) around an excited state fluorophore which is a function of the motional restriction imposed on the solvent molecules in the immediate vicinity of the fluorophore. Utilizing this approach, it becomes possible to probe the mobility parameters of the environment itself (which is represented by the relaxing solvent molecules) using the fluorophore merely as a reporter group. Further, since the ubiquitous solvent for biological systems is water, the information obtained in such cases will come from the otherwise “optically silent” water molecules. This makes REES and related techniques extremely useful since hydration plays a crucial modulatory role in a large number of important cellular events,<sup>21</sup> including lipid–protein interactions<sup>22</sup> and ion transport.<sup>23–25</sup> We have previously shown that REES and related techniques (wavelength-selective fluorescence approach) serve as a powerful tool to monitor organization and dynamics of probes and peptides bound to membranes or micelles.<sup>11,17,26–33</sup>

**Transmembrane Anisotropy.** The biological membrane is a highly organized molecular assembly, largely confined to two dimensions, and exhibits considerable degree of anisotropy along the axis perpendicular to the membrane plane. While the center of the bilayer is nearly isotropic, the upper portion, only a few angstroms away toward the membrane surface, is highly ordered.<sup>34–41</sup> As

a result, properties such as polarity, fluidity, segmental motion, ability to form hydrogen bonds, and extent of solvent penetration would vary in a depth-dependent manner in the membrane. A direct consequence of such an anisotropic transmembrane environment will be the differential extents to which the mobility of water molecules will be retarded at different depths in the membrane relative to the water molecules in bulk aqueous phase. We show here that, for a given fluorophore, both the magnitude of red-edge excitation shift (REES) and the dependence of fluorescence polarization and lifetimes on excitation and emission wavelengths, vary as a function of probe penetration depth. In particular, we demonstrate that REES of two anthroyloxy probes, namely 2- and 12-(9-anthroyloxy)stearic acid (2-AS and 12-AS, respectively), depend on their precise location in the membrane. This result correlates very well with differential rates of solvent relaxation at different depths in the membrane. This is further supported by very different rotational correlation times obtained for these two membrane probes.

## Experimental Section

**Materials.** Dioleoyl-*sn*-glycero-3-phosphocholine (DOPC) was purchased from Avanti Polar Lipids (Birmingham, AL). Dimyristoyl-*sn*-glycero-3-phosphocholine (DMPC) was obtained from Sigma Chemical Co. (St. Louis, MO). 2- and 12-AS were from Molecular Probes (Eugene, OR). DOPC was checked for purity by thin-layer chromatography on silica gel precoated plates (Sigma) in chloroform/methanol/water (65:35:5, v/v/v), and was found to give one spot with a phosphate-sensitive spray and on subsequent charring.<sup>42</sup> Concentration of DOPC was determined by phosphate assay after total digestion by perchloric acid.<sup>43</sup> DMPC was used as a standard to assess lipid digestion. Solvents used were of spectroscopic grade. Water was purified through a Millipore (Bedford, MA) Milli-Q system and used throughout.

**Preparation of Vesicles.** Two kinds of vesicles were used. All experiments involving steady-state fluorescence measurements were done using multilamellar vesicles (MLV) of DOPC containing 1% (mol/mol) 2- or 12-AS, as described previously.<sup>5</sup> In general, 320 nmol of DOPC in chloroform was mixed with 3.2 nmol of the probe in chloroform. A few drops of chloroform were added and mixed well, and the samples were dried under a stream of nitrogen while being warmed gently (~35 °C). After further drying under a high vacuum for at least 3 h, 1.5 mL of 10 mM sodium acetate, 150 mM sodium chloride, pH 5.0 buffer was added, and each sample was vortexed for 3 min to disperse the lipids. Background samples were prepared the same way except that the probes were omitted.

For experiments in which fluorescence lifetimes were measured, unilamellar vesicles (ULV) of DOPC labeled with 1% (mol/mol) 2- or 12-AS were prepared by the ethanol injection method.<sup>44</sup> For this, 1280 nmol of DOPC and 12.8 nmol of the fluorescent probe were dried together. The dried lipids were then dissolved in ethanol to give a final concentration of about 40 mM. This ethanolic lipid solution was then injected into 10 mM sodium acetate, 150 mM sodium chloride, and pH 5.0 buffer while

- (17) Mukherjee, S.; Chattopadhyay, A. *J. Fluorescence* **1995**, *5*, 237.  
 (18) Galley, W. C.; Purkey, R. M. *Proc. Natl. Acad. Sci. U.S.A.* **1970**, *67*, 1116.  
 (19) Demchenko, A. P. *Trends Biochem. Sci.* **1988**, *13*, 374.  
 (20) Lakowicz, J. R.; Keating-Nakamoto, S. *Biochemistry* **1984**, *23*, 3013.  
 (21) Haussinger, D. *Biochem. J.* **1996**, *313*, 697.  
 (22) Ho, C.; Stubbs, C. D. *Biophys. J.* **1992**, *63*, 897.  
 (23) Fischer, W. B.; Sonar, S.; Marti, T.; Khorana, H. G.; Rothschild, K. J. *Biochemistry* **1994**, *33*, 12757.  
 (24) Kandori, H.; Yamazaki, Y.; Sasaki, J.; Needleman, R.; Lanyi, J. K.; Maeda, A. *J. Am. Chem. Soc.* **1995**, *117*, 2118.  
 (25) Sankaramakrishnan, R.; Sansom, M. S. P. *FEBS Lett.* **1995**, *377*, 377.  
 (26) Chattopadhyay, A. *Biophys. J.* **1991**, *59*, 191a.  
 (27) Chattopadhyay, A.; Mukherjee, S. *Biochemistry* **1993**, *32*, 3804.  
 (28) Chattopadhyay, A.; Rukmini, R. *FEBS Lett.* **1993**, *335*, 341.  
 (29) Mukherjee, S.; Chattopadhyay, A. *Biochemistry* **1994**, *33*, 5089.  
 (30) Mukherjee, S.; Chattopadhyay, A.; Samanta, A.; Soujanya, T. *J. Phys. Chem.* **1994**, *98*, 2809.  
 (31) Guha, S.; Rawat, S. S.; Chattopadhyay, A.; Bhattacharyya, B. *Biochemistry* **1996**, *35*, 13426. Raja, S. M.; Rawat, S. S.; Chattopadhyay, A.; Lala, A. K. *Biophys. J.*, in press.  
 (32) Chattopadhyay, A.; Mukherjee, S.; Rukmini, R.; Rawat, S. S.; Sudha, S. *Biophys. J.* **1997**, *73*, 839.  
 (33) Rawat, S. S.; Mukherjee, S.; Chattopadhyay, A. *J. Phys. Chem. B* **1997**, *101*, 1922. Rawat, S. S.; Chattopadhyay, A. *J. Fluoresc.*, in press.

- (34) Seelig, J. *Q. Rev. Biophys.* **1977**, *10*, 353.  
 (35) Perochon, E.; Lopez, A.; Tocanne, J. F. *Biochemistry* **1992**, *31*, 7672.  
 (36) Ashcroft, R. G.; Coster, H. G. L.; Smith, J. R. *Biochim. Biophys. Acta* **1981**, *643*, 191.  
 (37) Stubbs, C. D.; Meech, S. R.; Lee, A. G.; Phillips, D. *Biochim. Biophys. Acta* **1985**, *815*, 351.  
 (38) White, S. H.; Wimley, W. C. *Curr. Opin. Struct. Biol.* **1994**, *4*, 79.  
 (39) Stubbs, C. D.; Ho, C.; Slater, S. J. *J. Fluoresc.* **1995**, *5*, 19.  
 (40) Venable, R. M.; Zhang, Y.; Hardy, B. J.; Pastor, R. W. *Science* **1993**, *262*, 223.  
 (41) Gawrisch, K.; Barry, J. A.; Holte, L. L.; Sinnwell, T.; Bergelson, L. D.; Ferretti, J. A. *Mol. Membr. Biol.* **1995**, *12*, 83.  
 (42) Dittmer, J. C.; Lester, R. L. *J. Lipid Res.* **1964**, *5*, 126.  
 (43) McClare, C. W. F. *Anal. Biochem.* **1971**, *39*, 527.  
 (44) Batzri, S.; Korn, E. D. *Biochim. Biophys. Acta* **1973**, *298*, 1015; Kremer, J. M. H.; Esker, M. W. J.; Pathmanoharan, C.; Wiersema, P. H. *Biochemistry* **1977**, *16*, 3932.

vortexing to give a final concentration of 0.85 mM lipid in the buffer.

**Steady-State Fluorescence Measurements.** Steady-state fluorescence measurements were performed with a Hitachi F-4010 spectrofluorometer using 1 cm path length quartz cuvettes. Excitation and emission slits with a nominal band-pass of 5 nm were used for all measurements. Background intensities of samples in which fluorophores were omitted were subtracted from each sample spectrum to cancel out any contribution due to the solvent Raman peak and other scattering artifacts. Fluorescence polarization measurements were performed using a Hitachi polarization accessory. Polarization values were calculated from<sup>45</sup>

$$P = \frac{I_{VV} - GI_{VH}}{I_{VV} + GI_{VH}} \quad (1)$$

where  $I_{VV}$  and  $I_{VH}$  are the measured fluorescence intensities with the excitation polarizer vertically oriented and the emission polarizer vertically and horizontally oriented, respectively.  $G$  is the grating correction factor and is equal to  $I_{HV}/I_{HH}$ . All experiments were done with multiple sets of samples and average values of fluorescence and polarization are shown in the figures. The spectral shifts obtained with different sets of samples were identical in most cases. In other cases, the values were within  $\pm 1$  nm of the ones reported.

**Time-Resolved Fluorescence Measurements.** Fluorescence lifetimes were calculated from time-resolved fluorescence intensity decays using a Photon Technology International (London, Ontario, Canada) LS-100 luminescence spectrophotometer in the time-correlated single photon counting mode. This machine uses a thyatron-gated nanosecond flash lamp filled with nitrogen as the plasma gas ( $16 \pm 1$  in. of mercury vacuum) and is run at 22–25 kHz. Lamp profiles were measured at the excitation wavelength using Ludox as the scatterer. To optimize the signal-to-noise ratio, 5000 photon counts were collected in the peak channel. All experiments were performed using slits with a nominal band-pass of 4 nm or less. The sample and the scatterer were alternated after every 10% acquisition to ensure compensation for shape and timing drifts occurring during the period of data collection. The data stored in a multichannel analyzer was routinely transferred to an IBM PC for analysis. Intensity decay curves were fitted as a sum of exponential terms:

$$F(t) = \sum_i \alpha_i \exp(-t/\tau_i) \quad (2)$$

$\alpha_i$  is a preexponential factor representing the fractional contribution to the time-resolved decay of the component with a lifetime  $\tau_i$ . The decay parameters were recovered using a nonlinear least squares iterative fitting procedure based on the Marquardt algorithm.<sup>46</sup> The program also includes statistical and plotting subroutine packages.<sup>47</sup> The goodness of the fit of a given set of observed data and the chosen function was evaluated by the reduced  $\chi^2$  ratio, the weighted residuals,<sup>48</sup> and the autocorrelation function of the weighted residuals.<sup>49</sup> A fit was considered acceptable when plots of the weighted residuals and the autocorrelation function showed random deviation about zero with a  $\chi^2$  value not more than 1.3. Mean (average) lifetimes  $\langle \tau \rangle$  for the biexponential decays of fluorescence were calculated from the decay times and preexponential factors using the following equation:<sup>50</sup>

$$\langle \tau \rangle = \frac{\alpha_1 \tau_1^2 + \alpha_2 \tau_2^2}{\alpha_1 \tau_1 + \alpha_2 \tau_2} \quad (3)$$

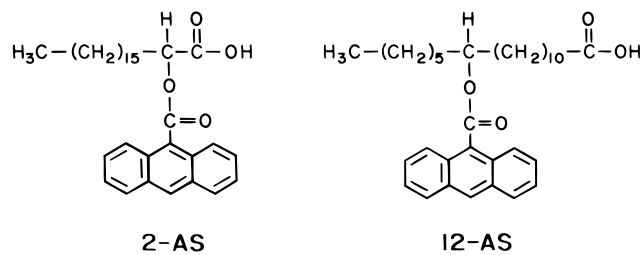


**Figure 1.** Chemical structures of 2- and 12-AS.

**Table 1.** Lifetimes of 2- and 12-AS in DOPC Vesicles as a Function of Excitation Wavelength<sup>a</sup>

excitation wavelength (nm)	$\alpha_1$	$\tau_1$ (ns)	$\alpha_2$	$\tau_2$ (ns)	$\langle \tau \rangle$ (ns)
(a) 2-AS					
365	0.56	8.88	0.44	3.23	7.62
380	0.65	8.75	0.35	3.82	7.81
390	0.63	8.29	0.37	2.37	7.44
395	0.65	8.21	0.35	2.44	7.41
400	0.51	8.20	0.49	1.50	7.20
(b) 12-AS					
365	0.74	13.95	0.26	6.02	12.91
380	0.83	13.61	0.17	5.43	12.99
390	0.71	14.00	0.29	7.49	12.83
395	0.65	14.44	0.35	8.35	12.99
400	0.75	13.91	0.25	6.26	12.91

<sup>a</sup> Emission wavelength: 460 nm.

All steady state as well as time-resolved fluorescence experiments were done at 23 °C.

## Results and Discussion

**Why Anthroyloxy Fatty Acids as Probes?** Fatty acids labeled with spectroscopic reporter groups have proved to be useful membrane probes (see ref 10 and references therein). The anthroyloxy fatty acids in which an anthracene group is attached by an ester linkage to various positions of an alkyl chain have been extensively used as fluorescent probes of micellar and bilayer structure.<sup>10,51–54</sup> These anthroyloxy fatty acids are extremely well suited for this study since they have been found to locate at a graded series of depths in the bilayer.<sup>10,52</sup> In fact, it has recently been shown that the depth of the anthroyloxy group is almost linearly related to the number of carbon atoms between it and the carboxyl group.<sup>9</sup> Depth analysis using the parallax method has previously shown that the anthroyloxy probes used by us (see Figure 1), 2-AS (the shallow probe) and 12-AS (the deep probe), have their anthroyloxy groups at 15.8 and 6.0 Å from the center of the bilayer at pH 5.0; i.e., these probes are  $\sim 10$  Å apart from each other in the bilayer.<sup>9</sup> Thus, they constitute one of the best calibrated sets of membrane probes available for membrane localization studies. In addition, the anthroyloxy probes are very well suited for wavelength-selective fluorescence studies because of relatively long fluorescence lifetimes (see Tables 1 and 2) and a large change in dipole moment upon excitation<sup>55</sup> (an important criterion for observation of REES, see ref 17) which results in a large Stokes' shift<sup>56</sup>

(45) Chen, R. F.; Bowman, R. L. *Science* **1965**, *147*, 729.

(46) Bevington, P. R. *Data Reduction and Error Analysis for the Physical Sciences*; McGraw-Hill: New York, 1969.

(47) O'Connor, D. V.; Phillips, D. *Time-Correlated Single Photon Counting*; Academic Press: London, 1984; p 180.

(48) Lampert, R. A.; Chewter, L. A.; Phillips, D.; O'Connor, D. V.; Roberts, A. J.; Meech, S. R. *Anal. Chem.* **1983**, *55*, 68.

(49) Grinvald, A.; Steinberg, I. Z. *Anal. Biochem.* **1974**, *59*, 583.

(50) Lakowicz, J. R. *Principles of Fluorescence Spectroscopy*; Plenum Press: New York, 1983.

(51) Tilley, L.; Thulborn, K. R.; Sawyer, W. H. *J. Biol. Chem.* **1979**, *254*, 2592.

(52) Villalain, J.; Prieto, M. *Chem. Phys. Lipids* **1991**, *59*, 9.

(53) Blatt, E.; Chigginio, K. P.; Sawyer, W. H. *Chem. Phys. Lett.* **1985**, *114*, 47.

(54) Hutterer, R.; Schneider, F. W.; Lanig, H.; Hof, M. *Biochim. Biophys. Acta* **1997**, *1323*, 195.

(55) Werner, T. C.; Hoffman, R. M. *J. Phys. Chem.* **1973**, *77*, 1611.

(56) Garrison, M. D.; Doh, L. M.; Potts, R. O.; Abraham, W. *Chem. Phys. Lipids* **1994**, *70*, 155.

**Table 2.** Lifetimes of 2- and 12-AS in DOPC Vesicles as a Function of Emission Wavelength<sup>a</sup>

emission wavelength (nm)	$\alpha_1$	$\tau_1$ (ns)	$\alpha_2$	$\tau_2$ (ns)	$\langle\tau\rangle$ (ns)
(a) 2-AS					
450	0.52	8.41	0.48	2.46	7.14
460	0.56	8.88	0.44	3.23	7.62
470	0.58	9.18	0.42	3.90	7.94
480	0.80	8.66	0.20	4.51	8.18
490	0.84	7.49	0.16	11.63	8.43
500	0.99	8.29	0.01	15.21	8.42
510	0.99	8.44	0.01	20.44	8.73
(b) 12-AS					
450	0.71	13.49	0.29	4.05	12.46
460	0.74	13.95	0.26	6.02	12.91
470	0.73	13.97	0.27	6.07	12.88
480	0.58	14.81	0.42	9.51	13.13
490	0.39	15.57	0.61	11.33	13.31
500	0.05	20.92	0.95	12.81	13.45
510	0.04	23.24	0.96	12.83	13.56

<sup>a</sup> Excitation wavelength 365 nm.

and makes their fluorescence sensitive to the immediate environment. All experiments have been done at pH  $\sim$  5.0 so that the anthroyloxy probes are in their protonated states and ground-state heterogeneity due to ionization of the carboxyl group is avoided.<sup>9,10</sup>

**The Red-Edge Effect.** In general, for a fluorophore in a bulk nonviscous solvent, the fluorescence decay rates and the wavelength of maximum emission are independent of the excitation wavelength. This is because of Kasha's rule which states that fluorescence normally occurs from the zero vibrational level of the first excited electronic state of a molecule.<sup>57</sup> However, this generalization breaks down in case of polar fluorophores in motionally restricted media such as very viscous solutions or condensed phases, that is, when the mobility of the surrounding matrix relative to the fluorophore is considerably reduced. Under such conditions, when the excitation wavelength is gradually shifted to the red edge of the absorption band, the maximum of fluorescence emission exhibits a concomitant shift toward higher wavelengths. Such a shift in the wavelength of maximum emission toward higher wavelengths, caused by a corresponding shift in the excitation wavelength toward the red edge of the absorption band, is termed the red-edge excitation shift or REES.<sup>17</sup> Since REES is observed only under conditions of restricted mobility, it serves as a faithful indicator of the dynamics of the fluorophore environment.

The origin of the red-edge effect lies in the change in fluorophore-solvent interactions in the ground and excited states, brought about by a change in the dipole moment of the fluorophore upon excitation, and the rate at which solvent molecules reorient around the excited-state fluorophore.<sup>17-20</sup> For a polar fluorophore, a dipolar interaction with the solvent molecules occurs in the ground state in order to minimize the energy of the given state. Since the dipole moment (magnitude as well as direction) of a molecule changes upon excitation, the solvent dipoles have to reorient around this new excited-state dipole moment of the fluorophore so as to attain an energetically favorable orientation. This readjustment of the dipolar interaction of the solvent molecules with the fluorophore essentially consists of two components: first, the redistribution of electrons in the surrounding solvent molecules because of the altered dipole moment of the excited-state fluorophore and then the physical reorientation of the

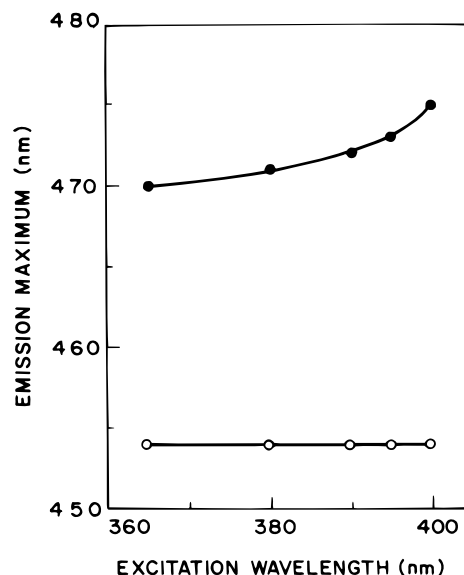


**Figure 2.** Effect of changing excitation wavelength on the wavelength of maximum emission for 2-AS (●) and 12-AS (○) in multilamellar vesicles of DOPC containing 1% (mol/mol) of the probe. See Experimental Section for other details.

solvent molecules around the excited-state fluorophore. The former process is almost instantaneous; i.e., electron redistribution in solvent molecules occurs on about the same time scale as the process of excitation of the fluorophore itself ( $10^{-15}$  s). The reorientation of the solvent dipoles, however, requires a net physical displacement. It is thus a much slower process and is dependent on the restriction to their mobility as offered by the surrounding matrix. More precisely, for a polar fluorophore in a bulk nonviscous solvent, this reorientation time ( $\tau_s$ ) is on the order of  $10^{-12}$  s, so that all the solvent molecules completely reorient around the excited-state dipole of the fluorophore well within its excited-state lifetime ( $\tau_F$ ), which is typically on the order of  $10^{-9}$  sec.<sup>58</sup> Hence, irrespective of the excitation wavelength used, all emission is observed only from the solvent-relaxed state. However, if the same fluorophore is now placed in a viscous medium, this reorientation process is slowed such that the solvent reorientation time is now of the order of  $10^{-9}$  s or longer. Under these conditions, excitation at the red edge of the absorption band selectively excites those fluorophores which interact more strongly with the solvent molecules in the excited state. These are the fluorophores around which the solvent molecules are oriented in a way similar to that found in the solvent-relaxed state. Thus, the necessary condition for REES is that different fluorophore populations are excited at the maximal and the red-edge excitation, and more importantly, this difference is maintained in the time scale of fluorescence lifetime. As discussed above, this requires that the dipolar relaxation time for the solvent shell be comparable to or longer than the fluorescence lifetime. This implies a reduced mobility of the fluorophore with respect to the surrounding matrix.

**Wavelength-Selective Fluorescence as a Membrane Dipstick.** The fluorescence emission maxima for 2- and 12-AS in DOPC vesicles are at 470 and 454 nm, respectively (see Figure 2). The blue shift of the emission

(57) Birks, J. B. *Photophysics of Aromatic Molecules*; Wiley-Interscience: London, 1970.

(58) Use of a single parameter  $\tau_s$  to describe the relaxation of solvent molecules is a first-order approximation since a set of relaxation times would exist in real systems. However, such an approximation is often made to make the relaxation model simple. Thus,  $\tau_s$  may be considered as a simple effective parameter characterizing the solvent relaxation process.

maximum for 12-AS (compared to 2-AS) is indicative of its deeper location in the nonpolar region of the membrane. The shifts in the maxima of fluorescence emission<sup>59</sup> of 2- and 12-AS in DOPC vesicles as a function of excitation wavelength are shown in Figure 2. As the excitation wavelength is changed from 365 to 400 nm, the emission maximum of 2-AS shifts from 470 to 475 nm, which amounts to a REES of 5 nm. Such shift in the wavelength of emission maximum with change in the excitation wavelength is characteristic of the red-edge effect and indicates that the anthroxyloxy moiety in 2-AS is localized in a motionally restricted region of the membrane that offers considerable resistance to solvent reorientation in the excited state. The emission maximum of 12-AS, however, does not change at all in this excitation range; i.e., 12-AS shows no REES. Thus, the magnitude of REES obtained for these probes varies in direct correlation with their penetration depths. In other words, whereas 2-AS, which is a shallow probe present in the membrane interfacial region, exhibits a REES of 5 nm, the deep probe 12-AS, present in the inner hydrocarbon-like region of the membrane, shows no REES. We attribute this to differential rates of solvent reorientation (which is a function of different degrees of motional restriction experienced by the solvent molecules) as a function of probe depth.

The red-edge effect originates from differential extents of solvent reorientation around the excited state fluorophore, with each excitation wavelength selectively exciting a different average population of fluorophores.<sup>17</sup> Since fluorescence lifetime serves as a faithful indicator for the local environment of a fluorophore and is sensitive to excited-state interactions, differential extents of solvent relaxation around a given fluorophore in the excited state could be expected to give rise to differences in its fluorescence lifetime. Table 1 shows the lifetimes of 2- and 12-AS in DOPC vesicles as a function of excitation wavelength, keeping the emission wavelength fixed at 460 nm in both cases. The fluorescence decays for 2- and 12-AS in DOPC vesicles fit to biexponential functions at all excitation and emission wavelengths, with mean lifetimes of ~7–8 and 12–13 ns, respectively. These values agree quite well with previous reports.<sup>60–62</sup> A typical decay profile with its biexponential fitting and the various statistical parameters used to check the goodness of the fit are shown in Figure 3.

When the excitation wavelength was gradually shifted toward the red edge of the absorption band (keeping the emission wavelength constant at 460 nm), it was found that the anthroxyloxy group in 2- and 12-AS exhibited very different behaviors. More precisely, whereas the mean fluorescence lifetime of 2-AS decreased from 7.62 to 7.20 ns (a total reduction of 5.5%) upon changing the excitation wavelength from 365 to 400 nm, no significant change was observed for 12-AS (see Table 1). Such a shortening of the mean lifetime of a fluorophore with increasing excitation wavelength in an environment of restricted mobility has previously been observed.<sup>11,17,27–29,33,63</sup> Since the emission wavelength is held constant at 460 nm (i.e.,

(59) We have used the term maximum of fluorescence emission in a somewhat wider sense here. In every case, we have monitored the wavelength corresponding to maximum fluorescence intensity, as well as the center of mass of the fluorescence emission. In most cases, both these methods yielded the same wavelength. In cases where minor discrepancies were found, the center of mass of emission has been reported as the fluorescence maximum.

(60) Matayoshi, E. D.; Kleinfeld, A. M. *Bioophys. J.* **1981**, *35*, 215.

(61) Chalpin, D. B.; Kleinfeld, A. M. *Biochim. Biophys. Acta* **1983**, *731*, 465.

(62) Squier, T. C.; Mahaney, J. E.; Yin, J. J.; Lai, C. S.; Lakowicz, J. R. *Bioophys. J.* **1991**, *59*, 654.

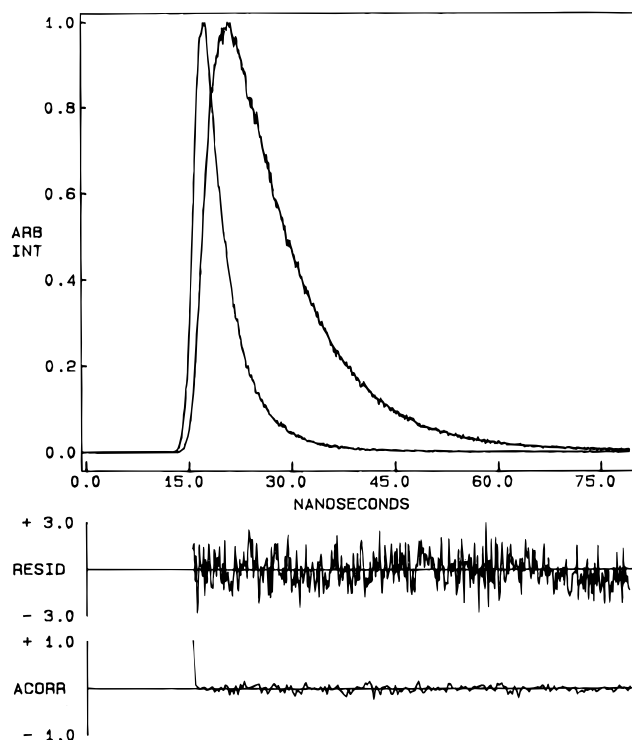
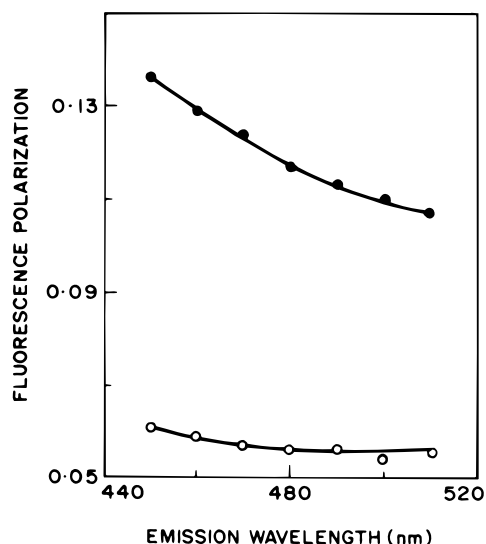


**Figure 3.** Time-resolved fluorescence intensity decay of 2-AS in unilamellar vesicles of DOPC. Excitation was at 365 nm and emission was monitored at 460 nm. The sharp peak on the left is the lamp profile. The relatively broad peak on the right is the decay profile, fitted to a biexponential function. The two lower plots show the weighted residuals and the autocorrelation function of the weighted residuals. Probe-to-lipid ratio was 1:100 (mol/mol). See Experimental Section for other details.

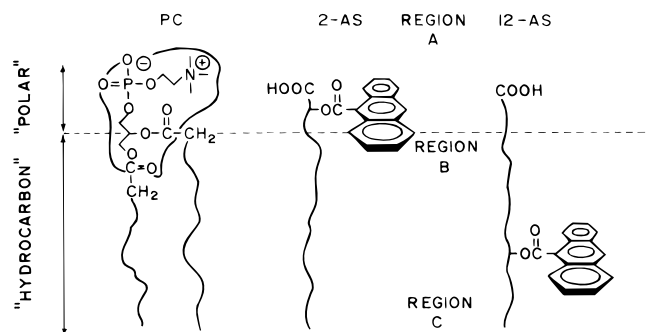
solvent reorientation has not been allowed to shift the emission wavelength toward higher wavelengths), the shortening of the mean lifetime of 2-AS could be attributed to the preselection of only that subpopulation of fluorophores (from a distribution of differentially solvated populations) that have emitted early.<sup>17,27</sup> Conversely, no such dependence of the fluorescence lifetime on excitation wavelength is observed in case of 12-AS, since the anthroxyloxy group in this case is localized in a much more fluid region of the membrane, so that the majority of the fluorophores have already attained the completely relaxed configuration prior to emission.

Table 2 shows the lifetimes of 2- and 12-AS in DOPC vesicles as a function of emission wavelength, keeping the excitation wavelength constant at 365 nm. As can be seen from this table, the lifetime of 2-AS increases from 7.14 to 8.73 ns (i.e., by 22.3%) with increasing emission wavelength from 450 to 510 nm. The corresponding increase in lifetime for 12-AS is much less (8.8%). This further demonstrates that the anthroxyloxy moiety of 2-AS is localized in a much more restricted environment compared to 12-AS, since such dependence of fluorescence lifetimes on emission wavelength have been previously reported for other fluorophores in environments of reduced mobility.<sup>11,17,27–29,33,60,64–66</sup> Such increasing lifetimes across the emission spectrum may be interpreted as emission predominantly from the relaxed fluorophores, which have spent enough time in the excited state in order to allow increasingly larger extents of solvent reorientation.

Such longer-lived fluorophores, which are also those which emit at higher wavelengths, should have more time to rotate in the excited state, giving rise to lower polarization. Figure 4 shows the variation in fluorescence polarization of 2- and 12-AS in DOPC vesicles as a function



**Figure 4.** Fluorescence polarization of 2-AS (●) and 12-AS (○) in multilamellar vesicles of DOPC as a function of emission wavelength. All other conditions are as in Figure 2. The excitation wavelength was 365 nm.



**Figure 5.** Schematic diagram of half of the membrane bilayer showing the localizations of the anthroyloxy groups of 2-AS and 12-AS at pH 5.0 in DOPC vesicles. The horizontal line at the bottom indicates the center of the bilayer. The membrane anisotropy along the axis perpendicular to the plane of the bilayer divides the membrane leaflet into three broad regions exhibiting very different dynamics. Region A: bulk aqueous phase, fast solvent relaxation; Region B: slow (restricted) solvent relaxation, hydrogen bonding (important for functionality), water penetration (interfacial water), highly anisotropic medium; Region C: bulk hydrocarbon-like environment, isotropic, fast solvent relaxation.

of wavelength across their emission spectrum. In general, polarizations are higher for 2-AS at all wavelengths than the corresponding values for 12-AS. This is again indicative of the differential localizations of these two anthroyloxy probes in the shallow interfacial region (motioally restricted) and deep (relatively fluid) regions of the membrane (see Figure 5). It is interesting to note that the polarization of 12-AS remains essentially invariant over the range of emission wavelengths. In sharp contrast to this, there is a considerable decrease in the polarization of 2-AS with increasing emission wavelength. The lowest polarization is observed toward the red edge where the relaxed emission predominates. Such markedly different dependences of 2- and 12-AS polarization on emission wavelengths thus further confirm the differential extents to which the water molecules around the anthroyloxy group in 2- and 12-AS are restricted by their immediate membrane environment.

**Table 3. Apparent Rotational Correlation ( $\tau_c$ ) Times for 2- and 12-AS in DOPC Vesicles**

membrane probe	$\tau_c$ (ns)
2-AS	67.83
12-AS	8.61

The apparent (average) rotational correlation times for 2- and 12-AS were calculated using Perrin's equation:<sup>50</sup>

$$\tau_c = \frac{\langle \tau \rangle r}{r_0 - r} \quad (4)$$

where  $r_0$  is the limiting anisotropy of the anthroyloxy probe,  $r$  is the steady-state anisotropy [derived from the polarization values using  $r = 2P/(3 - P)$ ], and  $\langle \tau \rangle$  is the mean fluorescence lifetime as calculated from eq 3. The values of the apparent rotational correlation times, calculated this way using a value of  $r_0$  of 0.1,<sup>67</sup> are found to be 67.83 and 8.61 ns for 2- and 12-AS, respectively, in DOPC vesicles (see Table 3). Thus, there is a reduction in apparent rotational correlation times along the axis perpendicular to the membrane bilayer. This reinforces our earlier conclusion that the motional restriction experienced by 2-AS is much more than that experienced by 12-AS.

Taken together, the above results point out that the same anthroyloxy group in 2- and 12-AS responds very differently to wavelength-selective fluorescence. The striking feature of these results is that the only difference in the fluorophore in these two cases is its localization in the membrane. More precisely, whereas the anthroyloxy group is located at the membrane interface in case of 2-AS, it is buried deep in the hydrocarbon-like interior of the membrane in 12-AS. The membrane interface (the region where the anthroyloxy group in 2-AS is located) is characterized by unique motional and dielectric characteristics different from the bulk aqueous phase and the more isotropic hydrocarbon-like deeper regions of the membrane.<sup>34-41</sup> This specific region of the membrane is also known to participate in intermolecular charge interactions,<sup>68</sup> and hydrogen bonding through the polar headgroup, or with interfacial water molecules<sup>69,70</sup> (see Figure 5). These structural features which slow solvent reorientation rates have been recognized as typical environmental features which give rise to appreciable red-edge effects.<sup>71</sup> On the other hand, when the anthroyloxy group is placed in the deeper hydrocarbon-like region of the membrane (as in the case of 12-AS), negligible red-edge effects are observed, because the environment is more isotropic and less restrictive. It is important to mention here that a number of observations point out that water penetrates to the deeper regions of the membrane bilayer<sup>35,39,72</sup> such as the region where the anthroyloxy group of membrane-bound 12-AS is localized.

(63) Demchenko, A. P. *FEBS Lett.* **1985**, *182*, 99.

(64) Badea, M. G.; DeToma, R. P.; Brand, L. *Biophys. J.* **1978**, *24*, 197.

(65) Lakowicz, J. R.; Bevan, D. R.; Maliwal, B. P.; Cherek, H.; Balter, A. *Biochemistry* **1983**, *22*, 5714.

(66) Demchenko, A. P.; Shcherbatska, N. V. *Biophys. Chem.* **1985**, *22*, 131.

(67) Tricerri, M. A.; Garda, H. A.; Brenner, R. R. *Chem. Phys. Lipids* **1994**, *71*, 61.

(68) Yeagle, P. *The Membranes of Cells*; Academic Press: Orlando, FL, 1987; p 89.

(69) Boggs, J. M. *Biochim. Biophys. Acta* **1987**, *906*, 353.

(70) Shin, T.-B.; Leventis, R.; Silvius, J. R. *Biochemistry* **1991**, *30*, 7491.

(71) Itoh, K.-I.; Azumi, T. *J. Chem. Phys.* **1975**, *62*, 3431.

(72) Meier, E. M.; Schummer, D.; Sandhoff, K. *Chem. Phys. Lipids* **1990**, *55*, 103; Stubbs, C. D.; Ho, C.; Slater, S. J. *J. Fluorescence* **1995**, *19*.

We conclude that wavelength-selective fluorescence constitutes a novel approach to probe defined depths in the membrane and can be conveniently used as a dipstick to characterize the depth of penetration of membrane-embedded fluorophores. One of the advantages of this approach is that the information obtained is dynamic in nature (in contrast to crystallographic information which is essentially static). This could prove to be a novel and

---

(73) Cornish, V. W.; Benson, D. R.; Altenbach, C. A.; Hideg, K.; Hubbell, W. L.; Schultz, P. G. *Proc. Natl. Acad. Sci. U.S.A.* **1994**, *91*, 2910; Nowak, M. W.; Kearney, P. C.; Sampson, J. R.; Saks, M. E.; Labarca, C. G.; Silverman, S. K.; Zhong, W.; Thorson, J.; Abelson, J. N.; Davidson, N.; Schultz, P. G.; Dougherty, D. A.; Lester, H. A. *Science* **1995**, *268*, 439.

powerful approach to probe environments in the vicinity of tryptophans (or other fluorescent residues, endogenous or introduced in a site-directed manner<sup>73</sup>) in membrane-bound probes and proteins.

**Acknowledgment.** We thank Y. S. S. V. Prasad, G. G. Kingi, and Satinder S. Rawat for technical help and Dr. R. Nagaraj for helpful discussions. This work was supported by the Council of Scientific and Industrial Research, Government of India. S.M. thanks the University Grants Commission for the award of a Senior Research Fellowship.

LA981553E